Available online at www.sciencedirect.com

SCIENCE DIRECT

Developmental Biology 284 (2005) 301 – 310

DEVELOPMENTAL BIOLOGY

www.elsevier.com/locate/ydbio

C. elegans HAM-1 positions the cleavage plane and regulates apoptosis in asymmetric neuroblast divisions

C. Andrew Frank[a,1], Nancy C. Hawkins[a,2], Catherine Guenther[a,3], H. Robert Horvitz[b], Gian Garriga[a,b,*]

[a]*Department of Molecular and Cell Biology, University of California, Berkeley, CA 94720-3204, USA*
[b]*Howard Hughes Medical Institute and Department of Biology, Massachusetts Institute of Technology, Cambridge, MA 02139, USA*

Received for publication 19 February 2005, revised 28 April 2005, accepted 18 May 2005
Available online 24 June 2005

Abstract

Asymmetric cell division occurs when a mother cell divides to generate two distinct daughter cells, a process that promotes the generation of cellular diversity in metazoans. During *Caenorhabditis elegans* development, the asymmetric divisions of neural progenitors generate neurons, neural support cells and apoptotic cells. *C. elegans* HAM-1 is an asymmetrically distributed cortical protein that regulates several of these asymmetric neuroblast divisions. Here, we show that HAM-1 is a novel protein and define residues important for HAM-1 function and distribution to the cell cortex. Our phenotypic analysis of *ham-1* mutant embryos suggests that HAM-1 controls only neuroblast divisions that produce apoptotic cells. Moreover, *ham-1* mutant embryos contain many unusually large cell-death corpses. An investigation of this corpse phenotype revealed that it results from a reversal of neuroblast polarity. A misplacement of the neuroblast cleavage plane generates daughter cells of abnormal size, with the apoptotic daughters larger than normal. Thus, HAM-1 regulates the position of the cleavage plane, apoptosis and mitotic potential in *C. elegans* asymmetric cell divisions.

Keywords: *Caenorhabditis elegans*; HAM-1; Asymmetric cell division; Neuroblast; Apoptosis

Introduction

Asymmetric cell division occurs when a mother cell generates two distinct daughter cells, a process that promotes the generation of cellular diversity in metazoans (Horvitz and Herskowitz, 1992). An important class of asymmetric cell division occurs in nervous system development when neuroblasts divide to produce daughter cells of distinct fate.

Asymmetric neuroblast divisions have been studied extensively in *Drosophila melanogaster*. In the *Drosophila* central nervous system (CNS), several asymmetrically localized molecules ensure the fidelity of neuroblast divisions. Three are found in a conserved complex: Bazooka (Baz; PDZ domain), DmPAR-6 (PDZ domain), and atypical protein kinase C (aPKC) (Petronczki and Knoblich, 2001; Wodarz et al., 2000). This complex recruits other factors, like Inscuteable (Insc) and Partner of Inscuteable (Pins), to the apical cortex of CNS neuroblasts. In turn, Insc and Pins direct the plane of cell division and the appropriate distribution of neuronal fate determinants, like Prospero or Numb (Kraut et al., 1996; Parmentier et al., 2000; Schaefer et al., 2000; Schober et al., 1999; Wodarz et al., 1999; Yu et al., 2000).

All *Caenorhabditis elegans* neurons are generated by asymmetric neuroblast divisions, but little is known about the molecular underpinnings of this process in the nem-

* Corresponding author. Department of Molecular and Cell Biology, University of California, 16 Barker Hall, Berkeley, CA 94720-3204, USA.
E-mail address: garriga@berkeley.edu (G. Garriga).
[1] Present Address: Department of Biochemistry and Biophysics, University of California, San Francisco, CA 94143-2822, USA.
[2] Present Address: Department of Molecular Biology and Biochemistry, Simon Fraser University, Burnaby, BC, Canada.
[3] Present Address: Department of Developmental Biology, Stanford School of Medicine, Stanford, CA 94305, USA.

0012-1606/$ - see front matter © 2005 Elsevier Inc. All rights reserved.
doi:10.1016/j.ydbio.2005.05.026

atode. We previously demonstrated that *ham-1* mutations disrupt several asymmetric neuroblast divisions, including the divisions of the two HSN/PHB neuroblasts (ABpl/rapppap) (Guenther and Garriga, 1996). In wild-type embryos, each HSN/PHB neuroblast divides asymmetrically to generate a smaller anterior daughter that undergoes programmed cell death and a larger posterior daughter, the HSN/PHB precursor, which subsequently divides to generate an HSN motor neuron and a PHB sensory neuron. In *ham-1* mutants, the anterior daughter can inappropriately survive, resulting in extra HSN and PHB neurons.

Unlike Numb and Prospero, HAM-1 does not behave like a cell-fate determinant. HAM-1 localizes to the posterior cortex of the HSN/PHB neuroblast and is inherited by the HSN/PHB precursor (Guenther and Garriga, 1996). Yet, it is the anterior HSN/PHB neuroblast daughter, the cell that normally does not inherit HAM-1, that is transformed in *ham-1* mutants.

In this study, we describe the role for HAM-1 in cell division. We identified six *ham-1* alleles that revealed residues of HAM-1 important for its function and localization. We observed that some apoptotic cells are abnormally large in *ham-1* mutants, a phenotype correlated with defects in asymmetric neuroblast division. We present evidence that this phenotype results from an altered cleavage plane in dividing neuroblasts. Our data suggest a mechanism by which HAM-1 could distribute developmental potential during asymmetric neuroblast divisions.

Materials and methods

C. elegans strains and genetics

Nematodes were maintained as described (Brenner, 1974). The wild-type strain N2 was used along with strains with the following genotypes: *Linkage Group* (*LG*) *I*: *ynIs45*[*flp-15::gfp*] (Li et al., 1999), *kyIs39*[*sra-6::gfp*] (Troemel et al., 1995); *LG II*: *gmIs20*[*hlh-14::gfp*] (Frank et al., 2003); *LG III*: *gmIs12*[*srb-6::gfp*] (Frank et al., 2003); *LG IV*: *ham-1(n1438)*, *ham-1(n1810)*, *ham-1(n1811)* (Desai et al., 1988), *ham-1(gm214)*, *ham-1(gm267)*, *ham-1(gm279)* (this study), *dpy-20(e1282)* (Hosono et al., 1982), *unc-30(e191)* (Brenner, 1974), *unc-31(e169)* (Brenner, 1974); *LG V*: *akIs7*[*nmr-1::gfp*] (Brockie et al., 2001); *LG X*: *gmIs18*[*ceh-23::gfp*] (Withee et al., 2004); extrachromosomal array: *gmEx285*[*nlp-1::gfp*] (Li et al., 1999).

Isolation of ham-1 mutants

Initial characterizations of *ham-1(n1438)*, *ham-1(n1810)*, and *ham-1(n1811)* have been described (Desai et al., 1988; Guenther and Garriga, 1996). *ham-1(gm214)*, *ham-1(gm267)*, and *ham-1(gm279)* were isolated in a genetic screen in which *gmIs12* worms were mutagenized with 50 mM EMS for 4 h, and mutants with extra GFP-positive PHB neurons were identified among the progeny of individual F1 hermaphrodites.

ham-1 cloning, gene structure, and rescue

ham-1 mapped genetically between RFLPs on the cosmids C08G1 and C13H6 on *LG IV*. The injection of the intervening cosmid C03F9 into *ham-1(n1811)* mutants rescued aspects of the Ham-1 phenotype. A 12 kb *Bst EII*/*Mlu I* subclone of C03F9 called p3F9M2 also rescued. DNA within this clone encodes the 1.8 kb *ham-1* mRNA.

The amplification of cDNAs using a primer complementary to SL1 (5′ TCTAGAATTCCGCGGTTTAATTACCCAAGTTTG 3′) and a second primer hm9 (5′ GCATGAAGCCCATGTAA 3′) demonstrated that the 5′ end of the *ham-1* transcript is generated by *trans*-splicing to SL1.

Identification of ham-1 lesions

The PCR primers Kg37 (5′ GCTTTCATTGTTTTTTCCAC 3′) and hm9 (5′ GCATGAAGCCCATGTAA 3′) yielded a 508 bp fragment from a wild-type genomic DNA template and a 270 bp fragment from a *ham-1(n1438)* template, revealing a 138 bp deletion in *ham-1(n1438)* mutants. For other lesions, the PCR primers ham-g1 (5′ TCCTTGTCTTCTCTCTCCGC 3′) and ham-g2 (5′ AGACACGTTTTGATGGGTGG 3′) were used to amplify genomic DNA from *ham-1* mutants. The sequencing primers hm8 (5′ CGAAGTGCATCTGCTCA 3′) and hm28 (5′ CGAGTGACCATCTGACA 3′) detected the *ham-1(n1810)*, *ham-1(n1811)*, *ham-1(gm267)*, and *ham-1(gm279)* lesions. The primer hm16 (5′ ATTCTGATGTGTTTGTGG 3′) detected the *ham-1(gm214)* lesion.

HAM-1 antibodies and immunostaining

HAM-1 antisera were obtained from rats and rabbits injected with the N-terminal half of HAM-1 as described previously (Guenther and Garriga, 1996). Antisera were affinity purified using an MBP-HAM-1 fusion generated from the vector pMALc. Mixed stage wild-type and *ham-1* embryos were immunostained as described (Guenther and Garriga, 1996).

Microscopy

Embryos were mounted on 5% agar pads in 2 μL of M9 and examined on a Zeiss Axioskop compound microscope. Images were captured with a Hamamatsu ORCA-ER digital camera and formatted using Adobe Photoshop.

We used anti-serotonin staining to detect HSNs in adult hermaphrodites (Garriga et al., 1993), anti-GABA staining to detect the RMEs (McIntire et al., 1992), the *srb-6::gfp* reporter *gmIs12* to detect both the PHA and PHB plasmid neurons (Troemel et al., 1995), the *nlp-1::gfp* reporter *gmEx285* to

detect PHBs (Li et al., 1999), the *flp-15::gfp* reporter *ynIs45* to detect the PHAs and I2 neurons (Li et al., 1999), and the *nmr-1::gfp* reporter *akIs7* to detect the AVA and RIM neurons (Brockie et al., 2001). We followed the divisions of the HSN/PHB neuroblasts by Nomarski optics and by GFP fluorescence using the *hlh-14::gfp* reporter *gmIs20* (Frank et al., 2003). Embryonic cells in the AVA/OLQsoV and the CEPso cell lineages were identified by Nomarski optics.

Additional cells that were not affected by *ham-1* mutations were: the GABAergic neurons AVL, DVB, DD and VD; the FMRFamidergic neurons VC and ALA; the serotonergic neurons ADF, NSM, RIG, RIH and I5; the dopaminergic neuron PDE; the *flp-15::gfp*-expressing neuron PHA; the *sra-6::gfp*-expressing neurons PVQ and ASH; the *nmr-1::gfp*-expressing neurons AVD, AVE AVG and PVC; the *ceh-23::gfp*-expressing neuron CAN; and the *mec-3::lacZ*-expressing neurons ALM and A/PVM. Taken together, only four of these neurons (A/PVM, NSM, PVD and PVQ) were derived from four lineages that contained an apoptopic cell that was either a sister or an aunt of the neuron scored. The other 18 unaffected neurons were derived from 18 lineages that lacked such a closely related apoptotic cell. Thus, of the 13 lineages that contained an apoptotic cell and where we scored the fate of a resulting neuron, nine were defective. The Ham-1 phenotype of the affected lineages can be explained by the apoptotic cell surviving and adopting the fate of its sister cell. By contrast, of the 18 lineages that lacked an apoptotic cell and where we scored the fate of a neuron in the lineage, *ham-1* mutations had no obvious effect.

Results and discussion

HAM-1 is a novel protein with distinct functional regions

We cloned *ham-1* by mapping it relative to polymorphisms and rescuing *ham-1* mutants with genomic DNA clones (see Materials and methods). In the *C. elegans* genome database, *ham-1* is identified as F53B2.6. HAM-1 is a 414-amino-acid protein with few homologs and no

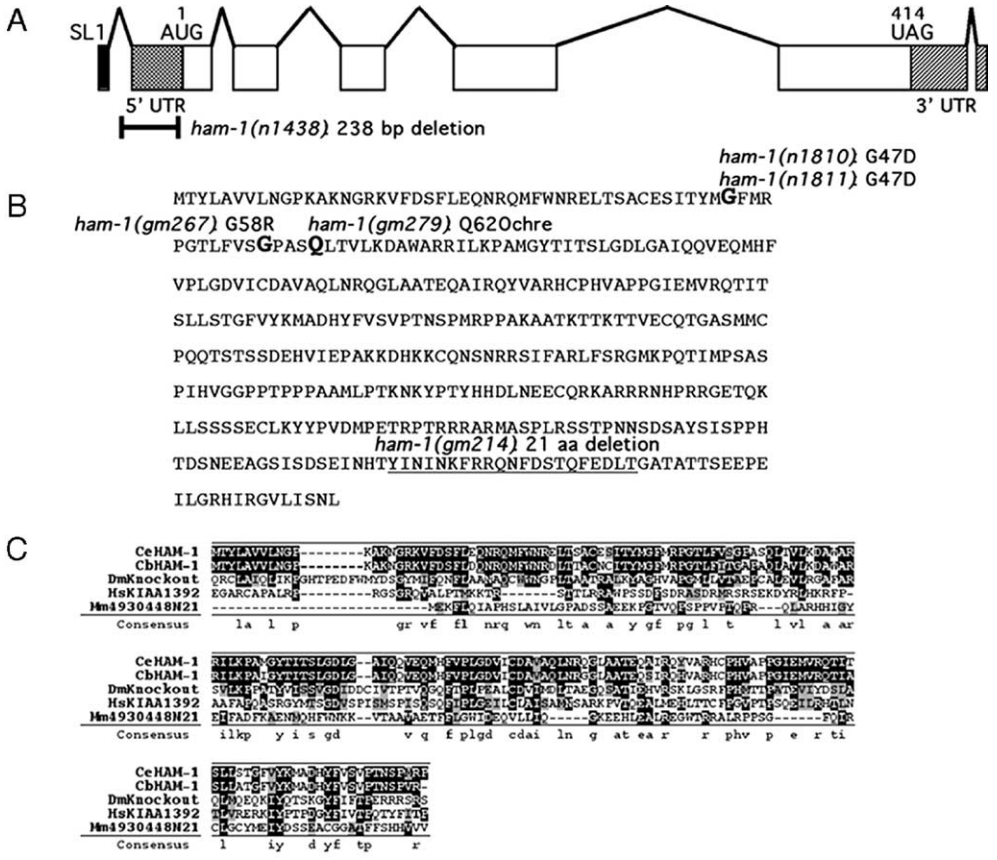

Fig. 1. *ham-1* gene structure, protein sequence, and homology. (A) Diagram of *ham-1* mRNA. The *ham-1*(*n1438*) lesion is a 238-base-pair deletion that removes sequences 65 nucleotides upstream of the *ham-1* SL1 *trans*-splice site to 12 nucleotides upstream of the predicted translational start site (AUG). (B) Primary sequence of HAM-1, a 414-amino-acid protein; additional lesions are shown. *ham-1*(*n1810*) and *ham-1*(*n1811*) are identical missense mutations, changing the glycine at residue 47 to aspartate. *ham-1(gm267)* changes the glycine at residue 58 to arginine. *ham-1(gm279)* is an ochre nonsense mutation. *ham-1(gm214)* is an in-frame deletion of 63 base pairs in exon 5, truncating HAM-1 by 21 amino acids (underlined). (C) A conserved region of HAM-1. HAM-1 has no known domains of conserved function. *C. elegans* HAM-1 (CeHAM-1) and *C. briggsae* HAM-1 (CbHAM-1) are 76% identical over their lengths. HAM-1 has an N-terminal similarity to the *D. melanogaster* protein Knockout (DmKnockout, accession NP_524193), as well as to human (HsKIAA1392, accession BAA92630) and mouse (Mm4930448N21, accession XP_134162) proteins of unknown function. Black shaded residues indicate identity. Gray shaded residues indicate similarity to corresponding black residues. Consensus residues are present in at least three of the five aligned sequences.

previously characterized domains (Fig. 1). Its closest homolog is *C. briggsae* HAM-1 (76% identical). An N-terminal stretch of HAM-1 (residues 15–170) is similar to *D. melanogaster* Knockout (Fig. 1), a protein involved in the innervation of larval muscles (Hartmann et al., 1997). This conserved stretch of HAM-1 is also similar to human and mouse sequences of unknown function (Fig. 1).

ham-1 was initially defined by the alleles *n1438*, *n1810*, and *n1811* based on an HSN migration phenotype (HSN abnormal migration) (Desai et al., 1988). We later demonstrated that *ham-1* mutations disrupt several asymmetric neuroblast divisions, including the ABpl/rapppap (HSN/PHB neuroblast) division (Guenther and Garriga, 1996). In wild-type embryos, the HSN/PHB neuroblast divides asymmetrically, generating a smaller anterior daughter that undergoes programmed cell death and a larger posterior daughter, the HSN/PHB precursor. The precursor then divides to produce the HSN motor neuron and the PHB sensory neuron (Sulston et al., 1983). In *ham-1* mutants, the anterior daughter can inappropriately survive, resulting in extra HSNs and PHBs (Guenther and Garriga, 1996). We isolated three *ham-1* alleles, *gm214*, *gm267* and *gm279*, in a screen for mutants with extra PHB neurons (Materials and methods; Fig. 1). *n1438* and *gm214* are deletion alleles that remove 5′ regulatory and 3′ coding sequences, respectively. *n1810*, *n1811* and *n267* are missense mutations in the conserved N-terminal domain. *gm279* is a nonsense mutation in codon 62 (Fig. 1).

Each *ham-1* allele reduces or eliminates gene function. All six mutations are recessive, generate similar phenotypes, and fail to complement one another (data not shown). Hemizygous *ham-1*/*sDf22* and homozygous *sDf22* animals have the same phenotype as homozygous *ham-1* mutants (Guenther and Garriga, 1996). *sDf22* is a deficiency that removes *ham-1* and flanking genes (Clark et al., 1988). Finally, *ham-1(n1438)* and *ham-1(gm279)* embryos, respectively, have severely reduced or no detectable HAM-1 protein (see below).

We stained the *ham-1* mutants with anti-HAM-1 antibodies to determine the effects of each mutation on HAM-1 protein expression and distribution. Prior immunostaining revealed that HAM-1 localizes to the cell periphery and is distributed asymmetrically in some embryonic cells, including the HSN/PHB neuroblast (Figs. 2A and B) (Guenther and Garriga, 1996). Two *ham-1* mutations, *gm279* and *n1438*, eliminate or strongly reduce HAM-1 expression. The *ham-1(gm279)* nonsense mutation eliminates all anti-HAM-1 staining in embryos (Fig. 2C), and no HAM-1 is detected on Western blots of *ham-1(gm279)* embryo extracts (Fig. 2G). *ham-1(n1438)* animals produce almost no HAM-

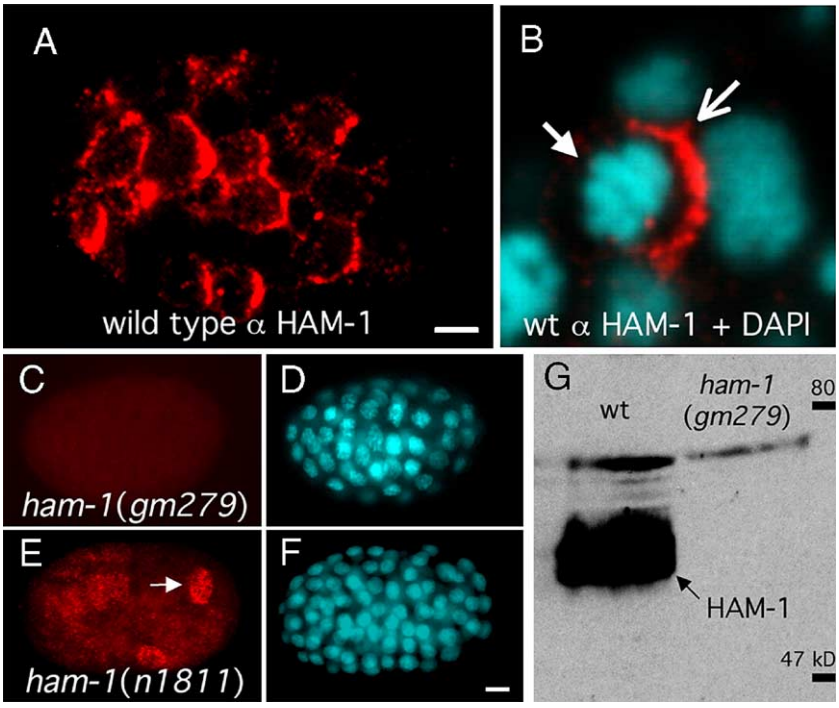

Fig. 2. HAM-1 protein expression in wild-type and *ham-1* embryos. Anti-HAM-1-stained embryos (A, C, E) and corresponding DAPI images to detect DNA (B, D, F). Anterior is to the left. (A) HAM-1 expression in a wild-type embryo. HAM-1 is at the cortex of many cells, sometimes in an asymmetric crescent and sometimes in a ring (Guenther and Garriga, 1996). Scale bar, 5 μm. (B) When HAM-1 (open arrow) is asymmetric, chromosomes (closed arrow) appear condensed, indicating that cells are mitotic. (C) Anti-HAM-1 staining of a *ham-1(gm279)* mutant. No HAM-1 is visible. (D) DAPI image of the *ham-1(gm279)* mutant embryo in panel C verifies that this embryo is at a stage in development when HAM-1 is normally detected. (E) Anti-HAM-1 staining in a *ham-1*(*n1811*) mutant. In *ham-1*(*n1810*) and *ham-1*(*n1811*) mutants, HAM-1 protein is mislocalized to the cytoplasm (arrow). (F) DAPI image of the *ham-1*(*n1811*) mutant embryo in panel E. Scale bar, 5 μm. (G) Anti-HAM-1 probed Western blot. Lanes on the corresponding protein gel were run using wild-type and *ham-1(gm279)* embryo extracts. HAM-1 is detected in the wild-type lane (wt), but not in the *ham-1(gm279)* lane.

1 protein (Guenther and Garriga, 1996). Northern analysis confirms that little *ham-1* mRNA is produced in *ham-1(n1438)* animals (data not shown). By contrast, HAM-1 is expressed in *ham-1(n1810)* and *ham-1(n1811)* mutants, but anti-HAM-1 staining showed that the mutant HAM-1(G47D) protein made in these embryos is localized inappropriately to the cytoplasm (Fig. 2E). *ham-1(gm214)* and *ham-1(gm267)* embryos have normal HAM-1 distribution (data not shown).

The cytoplasmic localization of HAM-1(G47D) in *n1810* and *n1811* mutant embryos suggests that the glycine at residue 47 is important for the cortical association of HAM-1. Notably, this glycine is conserved (Fig. 1C). Other HAM-1 regions are important for its function, independent of its localization, as evidenced by normal HAM-1 localization in *ham-1(gm214)* and *ham-1(gm267)* mutants.

Large apoptotic corpses in ham-1 mutants predict an altered division plane

In wild-type embryos, the HSN/PHB neuroblast generates an anterior daughter cell that undergoes programmed cell death and a larger posterior daughter, the HSN/PHB precursor (Fig. 3A) (Sulston et al., 1983). Sometimes, the anterior daughter does not die in *ham-1* mutants; instead, it becomes an extra HSN/PHB neuronal precursor (Guenther and Garriga, 1996). When the cell does die in *ham-1* mutants, the cell death corpse is aberrantly large (Fig. 3B).

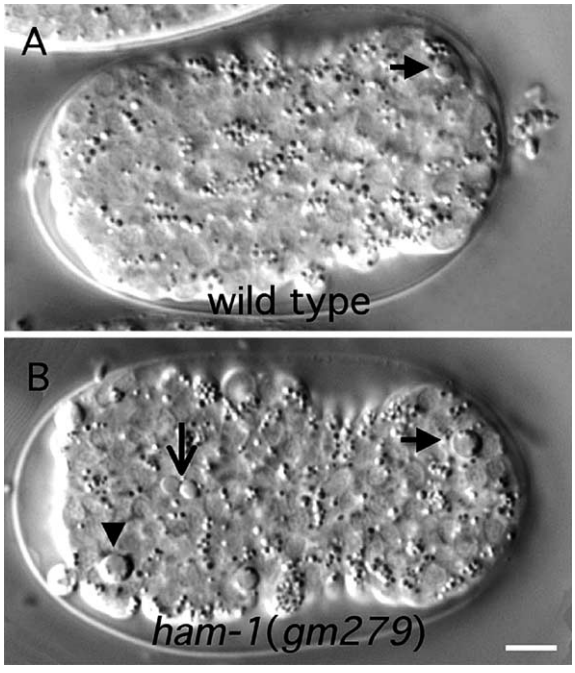

Fig. 3. *ham-1* embryos have large programmed cell death corpses. Nomarski images showing ventral views of (A) wild-type and (B) *ham-1(gm279)* embryos. Anterior is to the left. (A) The anterior daughter of the left HSN/PHB neuroblast (arrow) is undergoing programmed cell death and appears refractile. (B) A *ham-1(gm279)* mutant, in which this cell is dying. The dying cell appears much larger than normal (similar arrow). Other corpses in *ham-1* mutant embryos are also aberrantly large, such as the anterior daughter of the right AVA/OLQsoVR blast cell (ABalaappaaa) (arrowhead). The open arrow points to cell death corpses of normal size. Scale bar, 5 μm.

We wondered if this corpse appeared large in *ham-1* mutants because HAM-1 influences the position of the cleavage plane of some cell divisions. Perhaps, in the absence of *ham-1* function, an abnormally positioned division plane position can lead to abnormally sized daughter cells, and therefore, to corpses that are larger than normal.

To test this possibility, we utilized *hlh-14::gfp*, a reporter that expresses GFP in several neuroblasts, including the HSN/PHB neuroblast and its two daughters (Frank et al., 2003). In wild-type *hlh-14::gfp* embryos, the HSN/PHB neuroblast always divided to produce two unequally sized daughters. The anterior daughter, which normally dies, was smaller than its posterior sister, the HSN/PHB precursor. This size difference was readily detectable by GFP fluorescence (Figs. 4A, B, and C). In the absence of HAM-1 function, however, the sizes of the daughter cells were reversed; the anterior daughter cell was usually larger than its posterior sister (Figs. 4D, E and F).

To quantify size differences, we measured nuclear diameters using *hlh-14::gfp* (Figs. 4C and F). The nucleus occupies a large majority of the cell volume at this stage of *C. elegans* embryonic development. Therefore, the size of the nucleus corresponds to the size of the cell. In wild-type embryos, the anterior daughter nucleus was approximately 75% the diameter of the posterior daughter nucleus (Fig. 4E). By contrast, in *ham-1* embryos, this figure ranged from 97% in mutants carrying the weak loss-of-function allele *ham-1(gm267)* to 116% in strong loss-of-function mutants (Fig. 4G). We note that *ham-1(gm267)* is the weakest *ham-1* allele both by this assay and by the number of extra neurons produced (Table 1).

The HSN/PHB neuroblast daughters do not switch fates in ham-1 mutants

Because the relative sizes of the anterior and posterior HSN/PHB neuroblast daughters were reversed in *ham-1* mutants, we wondered whether their fates were also reversed. In particular, we wondered whether the posterior daughter, instead of the anterior daughter, died.

To test this possibility, the HSN/PHB neuroblast lineages of *hlh-14::gfp; ham-1(gm279)* embryos were examined. When one of the two HSN/PHB neuroblast daughters died, it was almost always the anterior daughter (7/8 cases). In these seven divisions, the anterior daughter nucleus was 114% the size of the posterior daughter nucleus, which is not different than the 115% scored for *hlh-14::gfp; ham-1(gm279)* when the fates of the daughter cells were not followed. Therefore, even though the anterior and posterior HSN/PHB neuroblast daughters showed size reversals in *ham-1* mutants, they did not appear to swap cell death/cell survival fates with great frequency. It is possible, however,

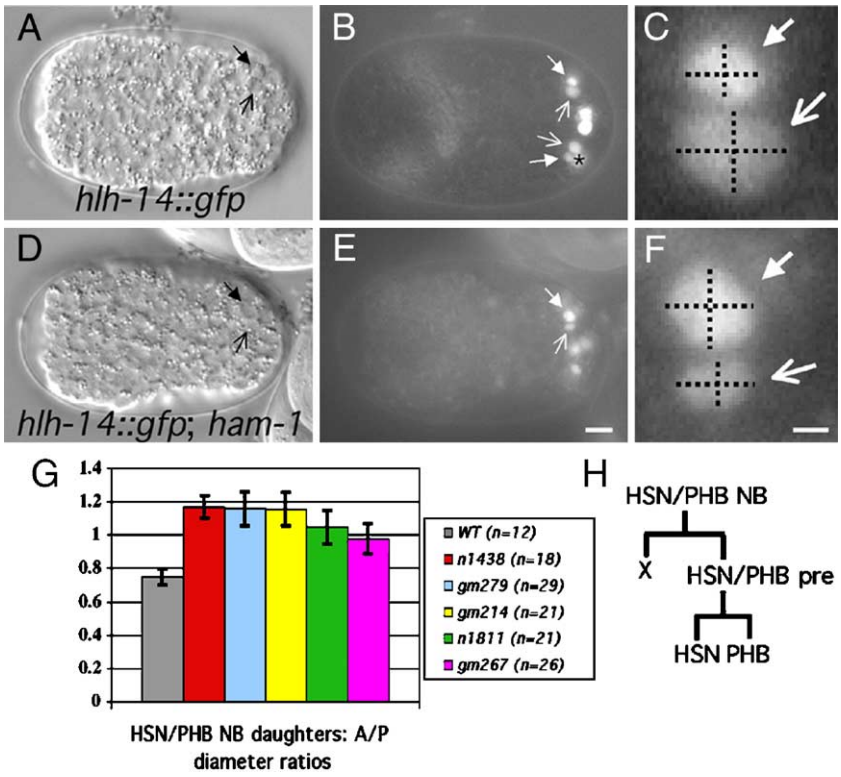

Fig. 4. HAM-1 positions the cleavage plane of the HSN/PHB neuroblast. (A–C) Wild-type and (D–F) *ham-1(gm279)* embryos carrying an *hlh-14::gfp* transgene, which expresses GFP in the daughters of the HSN/PHB neuroblast (Frank et al., 2003). Images show a ventral view, with anterior to the left. (A) Wild-type embryo expressing *hlh-14::gfp*. The left anterior HSN/PHB neuroblast daughter (closed arrow) and its sister cell, the left HSN/PHB precursor (open arrow), are shown. The anterior daughter appears refractile, executing its normal fate of programmed cell death. (B) GFP expression of the embryo in panel A. HLH-14::GFP is visible in the nuclei of the HSN/PHB neuroblast daughter cells on both the right and left sides. The anterior daughters (closed arrows) are smaller than their posterior sisters (open arrows). The asterisk covers cells out of this focal plane expressing GFP. The cells at the midline located between the cells of the HSN/PHB lineage may be the daughters of the neuroblast C.aapa (Frank et al., 2003). (C) Enlarged view of the left HSN/PHB neuroblast daughter nuclei. For each nucleus, the diameter was defined as the average of measurements along two orthogonal axes (dashed lines). (D) *ham-1(gm279)* embryo expressing HLH-14::GFP. The left anterior HSN/PHB neuroblast daughter (closed arrow) and its posterior sister cell (open arrow) are shown. (E) GFP expression in the embryo from panel D. The anterior daughter (closed arrow) is larger than its posterior sister (open arrow). As this is a slightly oblique view, the out-of-focus cells are descendants of the C.aapa and the right HSN/PHB neuroblasts. Scale bar, 5 μm. (F) Enlarged view of the left HSN/PHB neuroblast daughter nuclei from panel E, with arrows and lines analogous to those of panel C. Scale bar, 1 μm. (G) Relative diameters of the anterior and posterior HSN/PHB neuroblast daughter nuclei in wild-type and *ham-1* embryos. In wild-type embryos, the anterior daughter nucleus measures, on average, 75% of the diameter of the posterior daughter nucleus. In *ham-1*(*n1438*) embryos, the anterior daughter nucleus measures, on average, 116% of the diameter of the posterior daughter nucleus (compared to wild type, $P < 4.0 \times 10^{-18}$; Student's *t* test.). *ham-1*(*n1438*) is a strong loss-of-function allele. This ratio is 97% in embryos carrying a weak allele, *ham-1(gm267)* (compared to wild type, $P < 4.2 \times 10^{-12}$; *P* values for all *ham-1* alleles were smaller than this value; Student's *t* test.). Bars, ±SD. (H) HSN/PHB neuroblast lineage.

that a smaller size may influence the posterior HSN/PHB neuroblast daughter fate, as the single exception indicates. Such posterior daughter death may account for occasional missing HSNs and PHBs in *ham-1* mutants (Guenther and Garriga, 1996).

ham-1 mutations disrupt additional neuroblast divisions that generate apoptotic cells

We wondered whether the Ham-1 large-corpse phenotype occurred in other lineages affected by *ham-1* mutations. While examining the HSN/PHB neuroblast lineage, we noticed that *ham-1* mutant embryos have other large corpses, including one in the AVA/OLQsoV lineage (Fig. 3B). A neuroblast in this lineage produces a cell fated to die and a neural precursor that will divide to produce the AVA interneuron and a socket support cell for the OLQ sensory neuron (Sulston et al., 1983). If large corpses reflect defects in asymmetric cell division, *ham-1* mutants might have AVA neuron defects. To examine this possibility, we utilized *nmr-1::gfp*, a reporter that expresses GFP in the AVA neurons (Brockie et al., 2001). Consistent with our hypothesis, *nmr-1::gfp; ham-1* animals had extra AVA-like neurons (Table 1).

We demonstrated previously that *ham-1* mutants have extra neurons derived from the RID, ADL, ADE/ADA, PLM/ALN, and HSN/PHB lineages (Guenther and Garriga, 1996) (Fig. 5). With GFP reporter constructs and antibodies, we examined other neuronal lineages that generate cells that undergo programmed cell death (Fig. 5). In addition to the

Table 1
Extra neurons in *ham-1* mutants

Genotype	Frequency of extra neurons (number of sides examined)		
	HSN[a] [%]	PHB[b] [%]	AVA[c] [%]
Wild type	0 (100)	0 (100)	0 (68)
ham-1(n1438)	26 (98)	43 (102)	N/D
ham-1(gm279)	24 (90)	33 (202)	32 (44)
ham-1(gm214)	22 (32)	47 (110)	N/D
ham-1(n1811)	16 (58)	23 (274)	20 (15)
ham-1(gm267)	8 (64)	9 (186)	N/D
ced-3(n717)[d]	8 (26)	20 (84)	22 (9)
ham-1 ced-3[e]	100 (18)	93 (54)	100 (12)

N/D, not determined.
[a] HSN neurons stained with an anti-serotonin antibody in adults.
[b] *srb-6::gfp*-expressing PHB-like neurons in the tails of L1 larvae.
[c] *nmr-1::gfp*-expressing AVA-like neurons.
[d] The HSN/PHB lineage of *ced-3* mutants can produce an extra HSN-like neuron or an extra PHB-like neuron, but not both. This phenotype is distinct from the HSN/PHB lineage of *ham-1* mutants, which can produce both extra HSN-like and PHB-like neurons. Presumably, the surviving cell in *ced-3* has a limited potential to produce an HSN-like or PHB-like neuron.
[e] *ham-1*(*n1811*) *ced-3*(*n717*) was used for HSN and PHB; *ham-1*(*n1438*) *ced-3*(*n717*) was used for AVA.

AVA neurons, *nmr-1::gfp* expresses GFP in the RIM neurons (Brockie et al., 2001). Indeed, 2/15 sides examined in *ham-1(n1811)* animals had extra RIM-like neurons. The *flp-15::gfp* transgene expresses GFP in several neurons, including the I2 neurons (Li et al., 1999). We noticed that *flp-15::gfp; ham-1(gm279)* animals had extra I2-like neurons in 39/44 sides examined. Finally, we stained *ham-1(n1438)* mutants with anti-GABA antibodies and found that 12/15 animals had at least one extra RME-like neuron. The interpretation of this result is more complicated than that of the other lineages, which can be explained by an apoptotic cell surviving and adopting the fate of its sister cell. The four RME neurons are generated by three distinct lineages (Sulston, 1983). The RMEL/R neurons have sister cells that die and the RMEV neuron has an aunt that dies. The lineage that produces RMED, by contrast, lacks a closely related apoptotic cell. Because *ham-1* mutants produce no extra or missing ALA neurons, the RMED sister neuron, by anti-FMRFamide staining (Li and Calabrese, 1987) (unpublished observations), we conclude that either the RMEV or RMEL/R lineages or both lineages require HAM-1. Finally, we found that the aunt of the of the CEP socket cell produces an unusually large corpse (data not shown). While we have not shown that *ham-1* mutants produce extra CEPso cells, the large corpse phenotype shows that the lineage is affected, and we propose that this phenotype predicts the generation of extra CEPso cells.

All ten or eleven neuroblast lineages affected by *ham-1* mutations produced at least one apoptotic cell (Fig. 5). For each lineage except the CEPso lineage, which was scored as having abnormal corpses and not with CEPso markers, the Ham-1 phenotype can be explained by the apoptotic cell's survival and adoption of the fate of its sister. Does HAM-1 then specifically function in asymmetric cell divisions that generate apoptotic cells? Using a variety of cell markers to identify affected lineages, we have assayed 18 lineages that did not produce an apoptotic cell and found that none of these lineages produced extra or missing cells in *ham-1* mutants (Fig. 5; Materials and methods). By contrast, we assayed the fates of neurons from 14 lineages that produced an apoptotic cell and found that nine or ten produced extra neurons in *ham-1* mutants (Fig. 5; Materials and methods). Thus, while HAM-1 does not appear to regulate all asymmetric divisions that produce apoptotic cells, it appears to be specific for divisions that produce apoptotic cells in the lineages that we have assayed.

Could *ham-1*, therefore, simply act to promote the apoptosis of specific cells? Using mutations in the caspase gene *ced-3*, we previously showed that HAM-1 does not behave like a protein involved only in apoptosis (Guenther and Garriga, 1996). Strong *ced-3* loss-of-function mutations abolish all programmed cell deaths in *C. elegans* (Ellis and Horvitz, 1986; Yuan et al., 1993). However, the surviving anterior daughter of the HSN/PHB neuroblast only rarely adopts an HSN- or PHB-like fate in *ced-3* mutant embryos (Guenther and Garriga, 1996). Furthermore, *ham-1 ced-3* double mutants showed a striking increase in the number of extra neurons over *ham-1* or *ced-3* mutants alone (Guenther and Garriga, 1996) (Table 1). Thus, when the anterior HSN/PHB neuroblast daughter dies in *ham-1* mutants, it apparently has the potency to produce extra neurons, but this potency is masked by the fate of apoptosis. As with the HSN/PHB lineage, the extra-neuron phenotypes that we have observed in other lineages are also enhanced by the loss of *ced-3* (data not shown).

Division plane position and cell fate

What mechanisms regulate asymmetric cell division in HAM-1-dependent neuroblast lineages? Three classes of asymmetrically localized molecules have been implicated in asymmetric divisions: cell-fate determinants, molecules that distribute these determinants, and molecules that regulate both the distribution of cell-fate determinants and the orientation of the mitotic spindle. Because HAM-1 controls both cell fate and position of the cleavage plane, its function may be similar to that of the third class of molecules.

Of the proteins known to affect both asymmetric cell division and spindle position, some of the best characterized form the conserved PAR-3/PAR-6/PKC-3 complex (Kemphues et al., 1988; Tabuse et al., 1998; Watts et al., 1996). One function of this complex in *C. elegans* is to establish size asymmetry between AB and P1, the daughters of the *C. elegans* zygote. In wild-type embryos, the anterior daughter AB is larger than the posterior daughter P1, because the spindle is positioned posteriorly in the zygote. In the absence of *par-3*, *par-6*, or *pkc-3* function, AB and P1 are the same size because the spindle is not positioned asymmetrically.

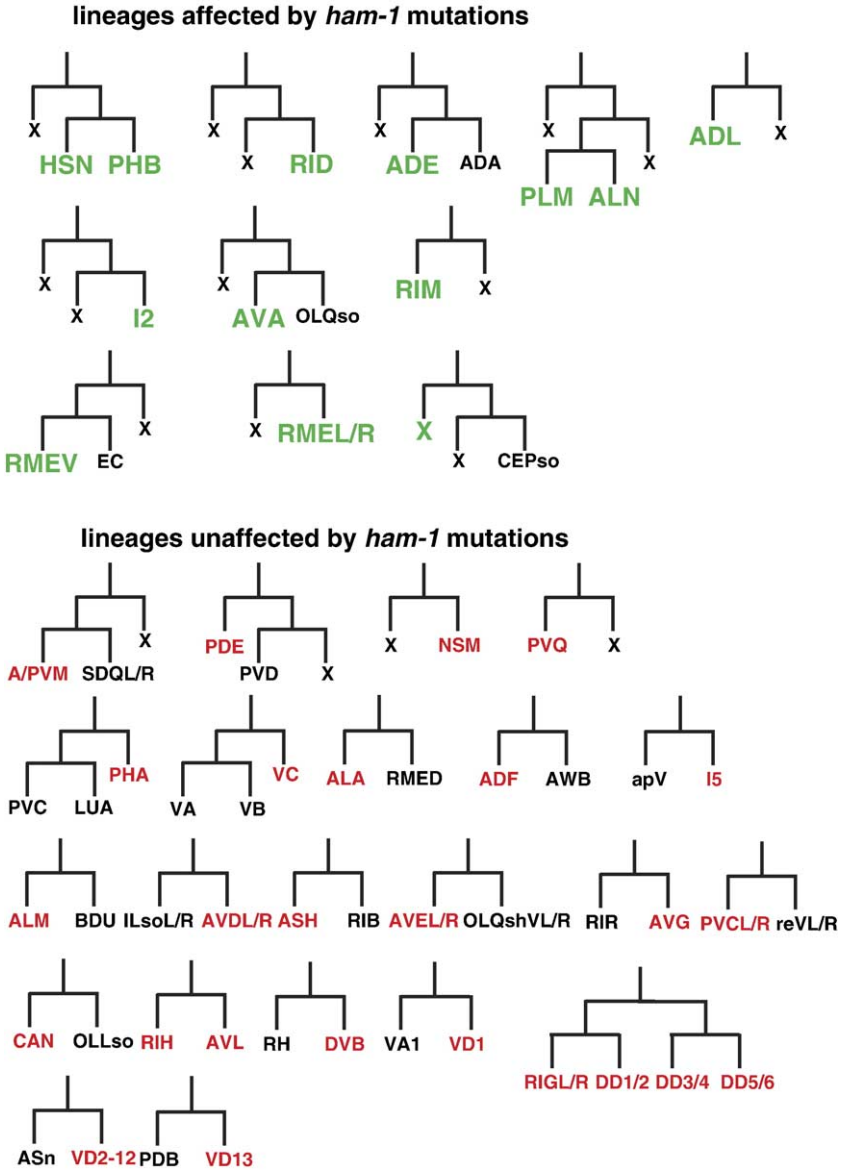

Fig. 5. Lineages that require HAM-1 function. The markers used to detect the cells described here are discussed in the Materials and methods section. Most of the lineages shown are bilaterally symmetric, and for most lineages, we have not labeled both bilaterally symmetric neurons in the diagrams. There are both left and right HSN and PHB neurons, for example, but we have labeled the neurons simply as HSN and PHB. When left and right neurons are labeled, it is because there are additional cells of this type. For example, there are four RME neurons: RMEL/R, RMEV and RMED. Lineages affected by *ham-1* mutations: The cells that were found to be abnormal in *ham-1* mutants are indicated in a large, green font. We previously identified five lineages (top line) that were affected by *ham-1* mutations. In this study, we identified three additional lineages that were affected by scoring the presence of extra neurons (middle line). We also found extra RME neurons in *ham-1* mutants, but could not determine whether the RMEV, RMEL/R or both lineages were affected (bottom line), so both lineages are shown. EC is our abbreviation for the excretory cell. Finally, we found that the dying aunt of the CEP socket cell is unusually large, consistent with a role for *ham-1* in this lineage. Lineages unaffected by *ham-1* mutations: The cells assayed are indicated in red type. The top line shows unaffected lineages that contain an apoptotic cell. Some neurons are generated by more than one lineage. The VD neurons, for example, are generated by three distinct lineages. apV and reV are our abbreviations for the ventral arc post V and rectal epithelial V cells, respectively.

In *Drosophila*, the homologous Baz(PAR-3)/DmPAR-6(PAR-6)/aPKC(PKC-3) complex is required to establish apical localization of the proteins Insc and Pins in CNS neuroblasts (Schober et al., 1999; Wodarz et al., 1999). Insc forms a crescent at the apical cortex and is needed for neuroblasts to divide in an apical/basal orientation (Kaltschmidt et al., 2000; Kraut and Campos-Ortega, 1996; Kraut et al., 1996). In the absence of Insc, neuroblasts divide in randomized orientations. Mammals also have homologs of PAR-3, PAR-6, and PKC-3, and these homologs are localized apically at tight junctions in epithelial cells. As one might expect, they influence epithelial polarity (Gao et al., 2002; Hirose et al., 2002; Suzuki et al., 2002; Suzuki et al., 2001; Yamanaka et al., 2001).

Like the PAR proteins, HAM-1 is localized asymmetrically in dividing cells and appears to position the cleavage

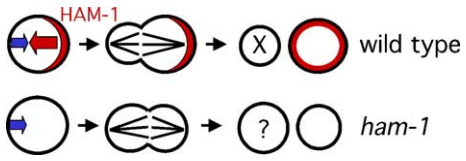

Fig. 6. Model for the role of HAM-1 in neuroblast division. Like the PARs in the *C. elegans* zygote, HAM-1 appears be important for the proper positioning of the mitotic spindle in dividing neuroblasts. HAM-1 (red) restricts the spindle to the anterior part of the cell (red arrow), leading to an anterior bias of the cleavage plane. In *ham-1* mutants, an opposing activity (blue) of unknown origin overcomes the absence of HAM-1, leading to a posterior bias of the cleavage plane. As a result, the anterior daughter is much larger than normal and often fails to express its normal cell death fate (? instead of X).

plane and, possibly as a consequence, to control the fates of the daughter cells. However, Ham-1 and Par phenotypes are distinct. In the HSN/PHB lineage, null *ham-1* mutations do not cause a symmetric division of the neuroblast as do the *par* mutations in the zygote. Instead, the division is still asymmetric in size, but reversed. The presence of many large cell corpses in *ham-1* embryos suggests that this cleavage phenotype is shared by many of the affected neuroblast divisions.

Our data suggest a model in which HAM-1 localizes to the posterior pole of the HSN/PHB neuroblast and restricts the mitotic spindle to the anterior side of the cell (Fig. 6). This asymmetric spindle position causes an anterior bias of the cleavage plane, generating a smaller anterior daughter and a larger posterior daughter. The reversal of the HSN/PHB neuroblast cleavage plane in *ham-1* mutants suggests that a second activity of unknown origin antagonizes the activity of HAM-1. In the absence of HAM-1, this second activity pushes the spindle to the posterior of the neuroblast (Fig. 6).

It is uncertain how HAM-1 regulates the spindle in neuroblasts. In the *C. elegans* zygote, heterotrimeric G-proteins appear to translate spatial information provided by the PARs to direct spindle position (Colombo et al., 2003; Gotta and Ahringer, 2001; Labbe et al., 2003). These G-proteins may signal through molecules that generate forces at the cortex and help position spindles, like dynein or microfilaments. As with HAM-1, a precise mechanism of how the PARs position the spindle is not yet clear.

Two general models can explain HAM-1's role in regulating cell fate. In one model, the cleavage plane position in neuroblasts would influence the inheritance of developmental potential. HAM-1's positioning of the cleavage plane affects the sizes of neuroblast daughters and, possibly, the inheritance of cell-fate determinants that are distributed asymmetrically by a HAM-1-independent mechanism. Posterior displacement of the cleavage plane in *ham-1* mutants could result in the inheritance by the anterior daughter of some of these determinants, allowing it to bypass its normal cell death fate and generate neurons instead. Studies of asymmetric divisions in the alga *Volvox carteri* indicate that the size of a daughter cell has a direct bearing on its fate (Kirk et al., 1993). Yet, while cell size might contribute to the fates of the HSN/PHB neuroblast daughter cells, it is not sufficient to specify the apoptotic fate. When a cell dies in the lineage, it is usually the anterior daughter even though it is the smaller daughter in wild-type embryos and the larger daughter in *ham-1* embryos. This observation favors another model in which HAM-1 distributes cell-fate determinants to daughter cells and independently regulates the position of the cleavage plane.

Acknowledgments

We thank members of the Garriga, Meyer, Kaplan, and Dernburg labs for helpful discussions. This work was supported by National Institutes of Health grants NS42213 to G.G. and GM24663 to H.R.H. H.R.H. is an Investigator of the Howard Hughes Medical Institute. N.C.H was supported by postdoctoral fellowships from the American Cancer Society and the American Heart Association. C.A.F. and C.G. were supported by National Science Foundation predoctoral fellowships.

References

Brenner, S., 1974. The genetics of *Caenorhabditis elegans*. Genetics 77, 71–94.

Brockie, P.J., Madsen, D.M., Zheng, Y., Mellem, J., Maricq, A.V., 2001. Differential expression of glutamate receptor subunits in the nervous system of *Caenorhabditis elegans* and their regulation by the homeodomain protein UNC-42. J. Neurosci. 21, 1510–1522.

Clark, D.V., Rogalski, T.M., Donati, L.M., Baillie, D.L., 1988. The unc-22(IV) region of *Caenorhabditis elegans*: genetic analysis of lethal mutations. Genetics 119, 345–353.

Colombo, K., Grill, S.W., Kimple, R.J., Willard, F.S., Siderovski, D.P., Gonczy, P., 2003. Translation of polarity cues into asymmetric spindle positioning in *Caenorhabditis elegans* embryos. Science 300, 1957–1961.

Desai, C., Garriga, G., McIntire, S.L., Horvitz, H.R., 1988. A genetic pathway for the development of the *Caenorhabditis elegans* HSN motor neurons. Nature 336, 638–646.

Ellis, H.M., Horvitz, H.R., 1986. Genetic control of programmed cell death in the nematode *C. elegans*. Cell 44, 817–829.

Frank, C.A., Baum, P.D., Garriga, G., 2003. HLH-14 is a *C. elegans* Achaete–Scute protein that promotes neurogenesis through asymmetric cell division. Development 130, 6507–6518.

Gao, L., Joberty, G., Macara, I.G., 2002. Assembly of epithelial tight junctions is negatively regulated by Par6. Curr. Biol. 12, 221–225.

Garriga, G., Desai, C., Horvitz, H.R., 1993. Cell interactions control the direction of outgrowth, branching and fasciculation of the HSN axons of *Caenorhabditis elegans*. Development 117, 1071–1087.

Gotta, M., Ahringer, J., 2001. Distinct roles for Galpha and Gbetagamma in regulating spindle position and orientation in *Caenorhabditis elegans* embryos. Nat. Cell Biol. 3, 297–300.

Guenther, C., Garriga, G., 1996. Asymmetric distribution of the *C. elegans* HAM-1 protein in neuroblasts enables daughter cells to adopt distinct fates. Development 122, 3509–3518.

Hartmann, C., Landgraf, M., Bate, M., Jackle, H., 1997. Kruppel target gene knockout participates in the proper innervation of a specific set of *Drosophila* larval muscles. EMBO J. 16, 5299–5309.

Hirose, T., Izumi, Y., Nagashima, Y., Tamai-Nagai, Y., Kurihara, H., Sakai,

T., Suzuki, Y., Yamanaka, T., Suzuki, A., Mizuno, K., Ohno, S., 2002. Involvement of ASIP/PAR-3 in the promotion of epithelial tight junction formation. J. Cell Sci. 115, 2485–2495.

Horvitz, H.R., Herskowitz, I., 1992. Mechanisms of assymetric cell division: two Bs or not two Bs, that is the question. Cell 68, 237–255.

Hosono, R., Hirahara, K., Kuno, S., Kurihara, T., 1982. Mutants of *C. elegans* with dumpy and rounded head phenotype. J. Exp. Zool. 224, 135–144.

Kaltschmidt, J.A., Davidson, C.M., Brown, N.H., Brand, A.H., 2000. Rotation and asymmetry of the mitotic spindle direct asymmetric cell division in the developing central nervous system. Nat. Cell Biol. 2, 7–12.

Kemphues, K.J., Priess, J.R., Morton, D.G., Cheng, N.S., 1988. Identification of genes required for cytoplasmic localization in early *C. elegans* embryos. Cell 52, 311–320.

Kirk, M.M., Ransick, A., McRae, S.E., Kirk, D.L., 1993. The relationship between cell size and cell fate in *Volvox carteri*. J. Cell Biol. 123, 191–208.

Kraut, R., Campos-Ortega, J.A., 1996. Inscuteable, a neural precursor gene of *Drosophila*, encodes a candidate for a cytoskeleton adaptor protein. Dev. Biol. 174, 65–81.

Kraut, R., Chia, W., Jan, L.Y., Jan, Y.N., Knoblich, J.A., 1996. Role of inscuteable in orienting asymmetric cell divisions in *Drosophila*. Nature 383, 50–55.

Labbe, J.C., Maddox, P.S., Salmon, E.D., Goldstein, B., 2003. PAR proteins regulate microtubule dynamics at the cell cortex in *C. elegans*. Curr. Biol. 13, 707–714.

Li, C., Calabrese, R.L., 1987. FMRFamide-like substances in the leech: III. Biochemical characterization and physiological effects. J. Neurosci. 7, 595–603.

Li, C., Nelson, L.S., Kim, K., Nathoo, A., Hart, A.C., 1999. Neuropeptide gene families in the nematode *Caenorhabditis elegans*. Ann. N. Y. Acad. Sci. 897, 239–252.

McIntire, S.L., Garriga, G., White, J., Jacobson, D., Horvitz, H.R., 1992. Genes necessary for directed axonal elongation or fasciculation in *C. elegans*. Neuron 8, 307–322.

Parmentier, M.L., Woods, D., Greig, S., Phan, P.G., Radovic, A., Bryant, P., O'Kane, C.J., 2000. Rapsynoid/partner of inscuteable controls asymmetric division of larval neuroblasts in *Drosophila*. J. Neurosci. 20, RC84.

Petronczki, M., Knoblich, J.A., 2001. DmPAR-6 directs epithelial polarity and asymmetric cell division of neuroblasts in *Drosophila*. Nat. Cell Biol. 3, 43–49.

Schaefer, M., Shevchenko, A., Knoblich, J.A., 2000. A protein complex containing inscuteable and the Galpha-binding protein Pins orients asymmetric cell divisions in *Drosophila*. Curr. Biol. 10, 353–362.

Schober, M., Schaefer, M., Knoblich, J.A., 1999. Bazooka recruits Inscuteable to orient asymmetric cell divisions in *Drosophila* neuroblasts. Nature 402, 548–551.

Sulston, J.E., 1983. Neuronal cell lineages in the nematode *Caenorhabditis elegans*. Cold Spring Harbor Symp. Quant. Biol. 48 (Pt. 2), 443–452.

Sulston, J.E., Schierenberg, E., White, J.G., Thomson, J.N., 1983. The embryonic cell lineage of the nematode *Caenorhabditis elegans*. Dev. Biol. 100, 64–119.

Suzuki, A., Yamanaka, T., Hirose, T., Manabe, N., Mizuno, K., Shimizu, M., Akimoto, K., Izumi, Y., Ohnishi, T., Ohno, S., 2001. Atypical protein kinase C is involved in the evolutionarily conserved par protein complex and plays a critical role in establishing epithelia-specific junctional structures. J. Cell Biol. 152, 1183–1196.

Suzuki, A., Ishiyama, C., Hashiba, K., Shimizu, M., Ebnet, K., Ohno, S., 2002. aPKC kinase activity is required for the asymmetric differentiation of the premature junctional complex during epithelial cell polarization. J. Cell Sci. 115, 3565–3573.

Tabuse, Y., Izumi, Y., Piano, F., Kemphues, K.J., Miwa, J., Ohno, S., 1998. Atypical protein kinase C cooperates with PAR-3 to establish embryonic polarity in *Caenorhabditis elegans*. Development 125, 3607–3614.

Troemel, E.R., Chou, J.H., Dwyer, N.D., Colbert, H.A., Bargmann, C.I., 1995. Divergent seven transmembrane receptors are candidate chemosensory receptors in *C. elegans*. Cell 83, 207–218.

Watts, J.L., Etemad-Moghadam, B., Guo, S., Boyd, L., Draper, B.W., Mello, C.C., Priess, J.R., Kemphues, K.J., 1996. par-6, a gene involved in the establishment of asymmetry in early *C. elegans* embryos, mediates the asymmetric localization of PAR-3. Development 122, 3133–3140.

Withee, J., Galligan, B., Hawkins, N., Garriga, G., 2004. *Caenorhabditis elegans* WASP and Ena/VASP proteins play compensatory roles in morphogenesis and neuronal cell migration. Genetics 167, 1165–1176.

Wodarz, A., Ramrath, A., Kuchinke, U., Knust, E., 1999. Bazooka provides an apical cue for inscuteable localization in *Drosophila* neuroblasts. Nature 402, 544–547.

Wodarz, A., Ramrath, A., Grimm, A., Knust, E., 2000. *Drosophila* atypical protein kinase C associates with Bazooka and controls polarity of epithelia and neuroblasts. J. Cell Biol. 150, 1361–1374.

Yamanaka, T., Horikoshi, Y., Suzuki, A., Sugiyama, Y., Kitamura, K., Maniwa, R., Nagai, Y., Yamashita, A., Hirose, T., Ishikawa, H., Ohno, S., 2001. PAR-6 regulates aPKC activity in a novel way and mediates cell–cell contact-induced formation of the epithelial junctional complex. Genes Cells 6, 721–731.

Yu, F., Morin, X., Cai, Y., Yang, X., Chia, W., 2000. Analysis of partner of inscuteable, a novel player of *Drosophila* asymmetric divisions, reveals two distinct steps in inscuteable apical localization. Cell 100, 399–409.

Yuan, J., Shaham, S., Ledoux, S., Ellis, H.M., Horvitz, H.R., 1993. The *C. elegans* cell death gene ced-3 encodes a protein similar to mammalian interleukin-1 beta-converting enzyme. Cell 75, 641–652.